JOURNAL OF OPTOELECTRONICS AND ADVANCED MATERIALS Vol. 12, No. 11, November 2010, p. 2236 - 2241

Electronic Structure of 18*R*-SnS$_2$ crystal

D. I. BLETSKAN*, V. V. FROLOVA, K. E. GLUKHOV
Uzhgorod National University, Voloshyn Str. 54, 88000 Uzhgorod, Ukraine

Calculations of energy band structure, total and partial densities of states and spatial valence charge distribution of 18*R* polytype of SnS$_2$ crystal are performed in the framework of the density functional theory (DFT). It was established The 18*R* polytype is shown to be an indirect-gap semiconductor (with $E_{gi}^{theor} = 1.18\ eV$) and the number of its valence states is shown to be by factor of nine larger than for the 2*H* polytype. The experimental data on the 18*R*-SnS$_2$ long-wavelength absorption edge studies are explained based on the energy band structure calculations and optical selection rules. The interlayer interaction in the 18*R* polytype was found to increase in comparison with the 2*H* polytype.

(Received November 10, 2010; November 19, 2010)

Keywords: Tin disulphide, polytypism, electronic band structure, density of states, selection rules, optical gap.

1. Introduction

Tin disulphide (SnS$_2$) belongs to the family of layered semiconductors of MX$_2$-type (M – metal, X – chalcogen) possessing a number of unique properties. A characteristic feature of the layered SnS$_2$ crystals is their polytypism, arising due to the infinite number of possible layer alternations which differ in the sequence of the constituent atoms. For instance, for SnS$_2$ the existence of more than 30 different polytypes had been shown, the most common being 2*H*, 4*H*, 6*H* and 18*R* [1-3] poltypes).

Possibilities of practical applications of Li intercalated layered SnS$_2$ crystals as a material for electrodes of the Li-batteries [4], SnS$_2$-SnSe$_2$-SnS$_2$ heterostructures, obtained by Van-der-Waals epitaxy [5], and nanostructurized tin disulphide [6] stimulate further studies of its properties which are determined by its spatial and energy structure. Most of the physical properties of semiconductors (optical and photoelectric properties, photoemission, photoluminescence, etc.) can be explained on the basis of their energy band structure in the *k*-space and the magnitudes of interband gaps in different points of the first Brillouin zone. A number of publications [7-16] have been devoted to the investigation of the nature of the absorption edge in tin disulphide layered crystals. The SnS$_2$ crystal band structure calculations have been carried out mostly for the 2*H* polytype and only in a single work [12] the calculation data for the energy band structure of 4*H* polytype were presented.

Meanwhile, it should be noted that at SnS$_2$ crystals growth from the gas phase by chemical gas transport the main fraction (up to 30 %) among the reaction products (except 2*H* and 4*H* polytypes) is the 18*R* polytype [3]. Nevertheless, it remains the less investigated one. Only fundamental absorption edge measurements [15,16] and Raman scattering studies [17] have been carried out for this crystal.

In the present work, in the framework of nonempirical *ab initio* method of DFT the calculations of the energy band structure, total and partial densities of states and spatial distribution of valence charge density in the 18*R* polytype of SnS$_2$ crystal are presented. 18*R*-SnS$_2$ crystal forms a trigonal lattice with parameters a = 3.6470 Å and c = 53.118 Å, Z = 9, space group $P\bar{3}ml$ [1, 2]. In the 18*R* polytype of tin dichalcogenides there are six different types of ‘sandwich’ arrangements and six different forms. At present, the only investigated structure is [1212]$_3$ (in Zhdanov's notation) with a $P\bar{3}ml$ (D_{3d}^3) space group, characterized by the following layer arrangement: $(A\gamma B)(A\beta C)(A\beta C)(B\alpha C)(B\gamma A)(B\gamma A)(C\beta A)(C\alpha B)(C\alpha B)$ [1,2] (Fig.1a).

The unit cell of the 18*R* polytype (Fig.1b) contains 27 atoms which belong to nine layers (for comparison, in the unit cell of 2*H* polytype there are only three atoms and they belong to a single layer). Each layer consists of two hexagonal dense packed layers built of edge-connected octahedra [SnS$_6$].

2. Calculation details

The energy structure calculations were carried out using ABINIT software package [18-20]; plane waves being used as a principal calculation basis. Translational invariance of the crystal was taken into account by periodical boundary conditions at the unit cell boundaries. The first principle normconserving atomic pseudopotentials [21] for the following electronic configurations were used for the calculation: [Kr]5$s^2$5p^2 (for Sn atoms), [Ne]3$s^2$3p^4 (for S atoms). The exchange-and-correlation interaction was taken into account in the framework of the local density approximation (LDA) [22]. Plane waves cut off energy for the self-consistent calculation was chosen as E_{cut} = 40 Ry in order to obtain the convergence in the total energy of the unit cell not worse than 0.001 Ry per atom. The plane wave basis consisted of about 20500 functions. The *k*-mesh density in the reciprocal space for the self-consistent calculation was also chosen based on similar considerations. Total and partial densities of states were calculated using the modified tetrahedron method, for which the energy

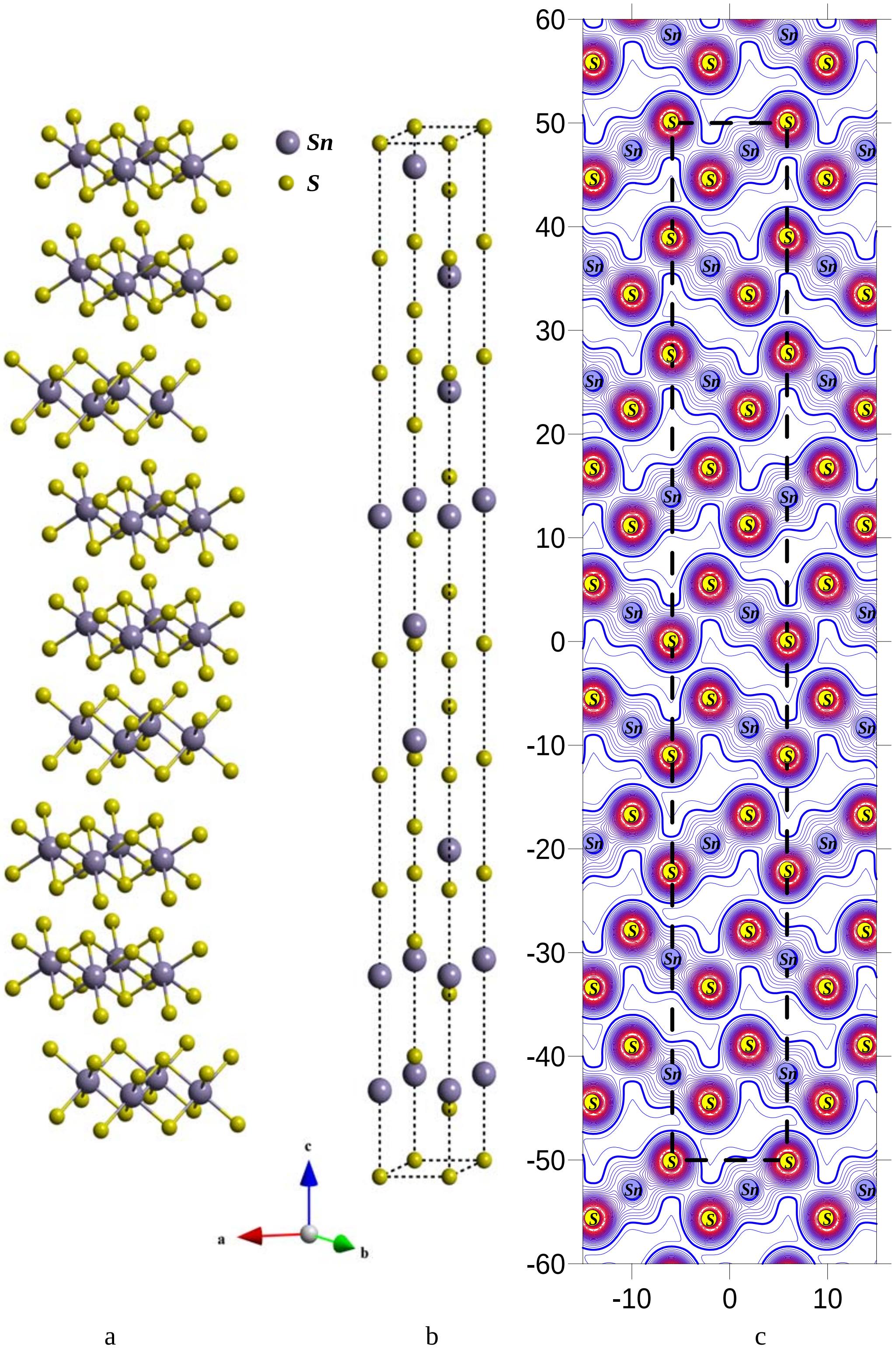

Fig.1 (a)- Crystalline structure, (b)- unit cell, and (c)- electron density map in the (110) plane of 18R-SnS_2.

states and the wave functions were calculated over a 21-point k-mesh. Integration over the Brillouin zone was performed using a method of special points on a 4x4x2 mesh in the reciprocal space [23]. All the calculations were carried out without taking into account spin-orbit interaction for structurally relaxed parameters of the crystal at zero temperature. The electron and hole effective masses were estimated numerically using the obtained set of E($\boldsymbol{k}$) points in the Brillouin zone by parabolic approximation of the dispersion curves in the vicinity of local extremum.

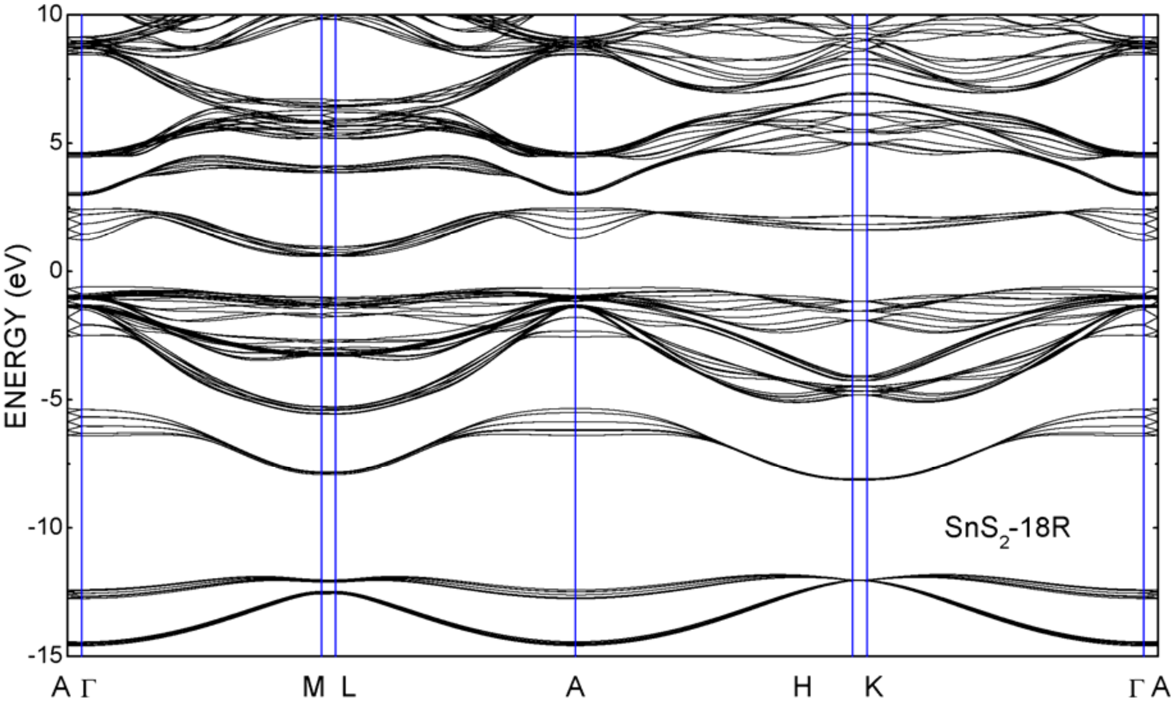

Fig.2 Dispersion branches E(k) in the Brillouin zone symmetrical points.

3. Analysis and discussion

The calculated energy band structure of 18*R*-SnS$_2$ crystal is shown in Fig. 2. Here the energy origin is set at the highest occupied state, i.e. at the top of the topmost valence band. The number of valence energy bands in the 18*R* polytype is by factor of 9 larger than that of the 2*H*-polytype, what is in agreement with the number of layers in the unit cell of this polytype (Fig.1b). 18*R* polytype, as well as 2*H* and 4*H* polytypes, is an indirect-gap semiconductor (the calculated value E_{gi} = 1.18 eV). The fundamental absorption edge of the layered 18*R*-SnS$_2$ crystal, obtained by chemical gas transport, was investigated in [16] in the temperature range 4.2–400 K. The authors of [16] also discussed the nature of the observed optical transitions (with the participation of phonons) in 18*R*-SnS$_2$ crystal, based on the calculated band structure [9] and the experimental Raman spectra [24] of 2*H* polytype of SnS$_2$ crystal what does not seem to be completely correct. From the analysis of the experimental absorption spectra it follows that the absorption edge is formed by indirect forbidden transitions with $\boldsymbol{E}\perp\boldsymbol{c}$ polarization and by direct allowed transitions with $\boldsymbol{E} \parallel \boldsymbol{c}$ polarization. It is also shown that the indirect transitions are two-phonon processes. The energy gap value at 300 K is 2.25 and 2.14 eV for $\boldsymbol{E}\perp\boldsymbol{c}$ and $\boldsymbol{E} \parallel \boldsymbol{c}$, respectively. Taking into account that the calculated gap value is approximately half of the experimentally obtained one (this is a common rule for DFT calculations based on LDA), for comparison of the theoretically calculated energy states with the optical transition energies one should perform a rigid shift of the conduction band. The value of this shift is determined from the experimental data and the selection rules for the indirect optical transitions. The symmetry analysis of the wave functions in the vicinity of the energy gap in Γ and M high-symmetry points of the Brillouin zone enables one to determine that the top of the valence band is formed by Γ_4 and M_2 states, while the bottom of the conduction band is described by Γ_1 and M_1 irreducible representations. So, the experimentally observed $\boldsymbol{E} \parallel \boldsymbol{c}$ indirect allowed transition can be identified as a transition $\Gamma_4 \rightarrow M_1$ from the valence band to conduction band with the participation of phonon with M_1^{ph} (Fig.3).

So, for the agreement of the calculated band structure with the optical transition experimental energy values the rigid shift of the conduction band should be ΔE = 0.96 eV. After the conduction band shift, the energies of other optical transitions were determined (Fig.3). A negligible difference between the experimental ($E_{gi}^{\exp}(\mathbf{E}\perp\mathbf{c}) = 2.25\,eV$) and theoretically calculated ($E_{gi}^{theor}(\mathbf{E}\perp\mathbf{c}) = 2.54\,eV$) energy values for the indirect forbidden transition can be caused by two factors: localization of bands extrema not directly in the high symmetry points but in their vicinity and ignoring of the temperature in our calculations.

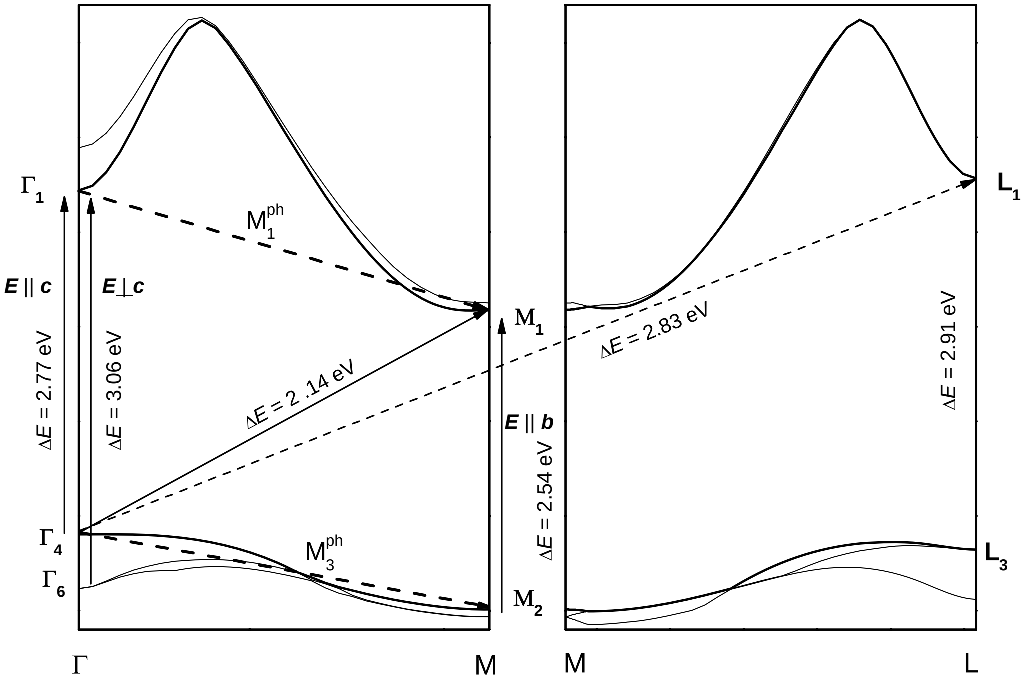

Fig.3 Selection rules for indirect optical transitions in the energy band spectrum of 18R-SnS$_2$. (The vertical arrows denote the transitions, allowed at the given polarization).

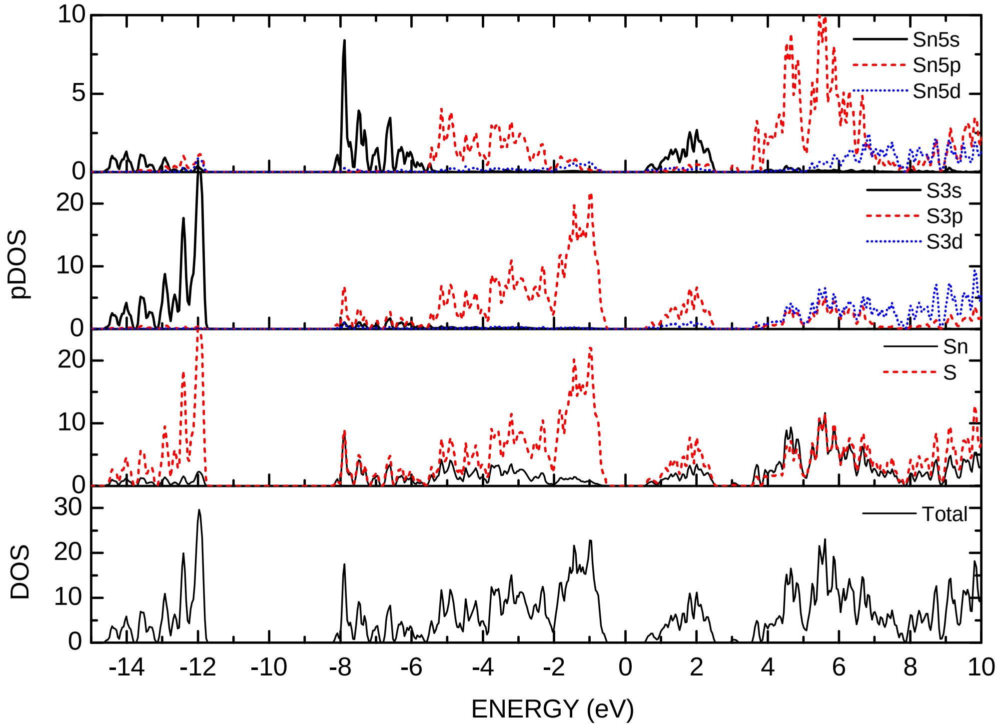

Fig. 4. Total and partial densities of states of 18R-SnS$_2$.

The calculated total (DOS) and partial (pDOS) density of states in valence and conduction bands are shown in Fig.4. In accordance with the calculation, the valence band of 18*R* polytype consists of three occupied energy subbands which are separated by a gap. In a common treatment, the lowest valence subband ((-12÷-15) eV) is formed by 3*s*-orbitals of S with an admixture of 5*s*- and 5*p*-states of tin. The middle valence subband ((-5.5÷ -8) eV) is formed mainly by 5*s* tin orbitals and 3*p* sulphur states. The upmost valence subband ((0÷ -5) eV) is formed by 3*p* sulphur states and 5*p* tin states. Note that the contribution of 3*p* states of sulphur in the valence band top formation is predominant. The bottom of the conduction band is formed by 5*s* states of tin and 3*p* states of sulphur.

Table 1 Structural and electronic parameters of 2H and 18R polytypes of SnS_2 crystal. Several values, indicated in some cells regarding 18R-SnS_2 crystal, are related to the presence of many different nonequivalent layers.

Parameter	2*H*-SnS_2	18*R*-SnS_2
a, Å	3.682	3.643
c, Å	5.830	53.05
d(Sn-S), Å	2.598	2.55918/2.55990/2.56003
d(S-S), Å	3.55015	3.6197/3.65743/3.65742
ρ(Sn-S)	0.226	0.233/0.231
ρ(S-S)	0.001	0.001/0.002
q(Sn)	3.072	3.072/3.080
q(S)	6.465	6.466/6.463/6.462/6.460/6.459
m_c/m_0	0.545	3.573
m_v/m_0	-0.748	-23.21

The calculated electron density enables the spatial distribution of the electron density over the unit cell to be mapped and the distribution character in the same crystallographic planes to be compared for different polytypes. A 2D map of the calculated density of the valence electron charge for the (110) crystallographic plane in 18*R* polytype is shown in Fig.1c: the lines connect the points of equal density values, the minimal density value $\rho_{min} = 0$; the difference between the two neighboring lines is $\Delta\rho = 5\cdot10^{-3}$ el./Bohr^3; the maximal value of the density is limited by $\rho_{max} = 1.8\cdot10^{-1}$ el./Bohr^3. Since the interatomic binding energy value depends on the electron density in the interatomic space, the higher density corresponds to a stronger binding. The distribution of the electron density over the unit cell is anisotropic, which is in the agreement with the layered structure of the material.

The calculated parameters of crystalline and electronic structure of the 2*H*- and 18*R*-SnS_2 crystals are compared in Table 1. Mulliken population analysis enables the values of effective charges on tin and sulphur atoms to be determined and the values of their orbital overlap to be calculated. As follows from table, the cation charge variation in both polytypes is small. Meanwhile, the charges on sulphur atoms undergo greater disturbances what is possibly related to the difference in their local environment in different layers. The values of electron and hole effective masses in the band extrema vicinity for both modifications of SnS_2 are also presented in the table. The considerable effective mass values for the 18*R* polytype indicate a weak dispersion of the energy branches, which is typical for layered materials. The increase of the effective masses in comparison with 2*H*-SnS_2 crystal is a manifestation of the crystal anisotropy increase.

References

[1] D. I. Bletskan, "Crystalline and glassy chalcogenides of Si, Ge, Sn and alloys on their base," Vol. 1, Zakarpattia, Uzhhorod, 2004.

[2] B. Palosz, W. Steurer, H. Schulz, Acta Crystallographia B., **46**, 499 (1990).

[3] T. Minagawa, Journal of Physical Society Japan, **49**, 2317 (1980).

[4] J. Morales, C. Perez-Vicente, J. L. Tirado, Solid State Ionies, **51**, 133 (1992).

[5] R. Schlaf, C. Pettenkofer, W. Jaegermann, Journal of Applied Physics, **85**, 6550 (1999).

[6] C. R. Wang, K. B. Tang, Q. Yang, Y. T. Qian, C. Y. Xu, Chemistry Letters, **30** 1294 (2001).

[7] M. Au-Yang, M. L. Cohen, Physical Review B., **178**, 1279 (1969).

[8] C. Y. Fong, M. L. Cohen, Physical Review B., **5**, 3095 (1972).

[9] I. Ch. Schlüter, M. Schlüter, Physica Status Solidi (b), **57**, 145 (1973).

[10] R. B. Murray, R. H.Williams, Journal of Physics C: Solid State Physics, **6**, 3643 (1973).

[11] J. Bordas, J. Robertson, A. Jakobsson, Journal of Physics C: Solid State Physics, **11**, 2607 (1978).

[12] M. J. Powell, E. A. Marseglia, W. Y. Liang, Journal of Physics C: Solid State Physics, **11**, 895 (1978).

[13] M. J. Powell, Journal of Physics C: Solid State Physics, **10**, 2967 (1977).

[14] G. Domingo, R. S. Itoga, C. R. Kannewurf, Physical Review B., **143**, 536 (1966).

[15] R. Bacewicz, B. Palosz, W. Palosz, S. Gierlotka, Solid State Communications, **54**, 283 (1985).

[16] H. Nozaki, I. Imai, Physica B., **105**, 74 (1981).

[17] S. Nakashima, H. Katahama, A. Mitsuishi, Physica B., **105**, 343 (1981).

[18] X. Gonze, J.-M. Beuken, R. Caracas, F. Detraux, M. Fuchs, G.-M. Rignanese, L. Sindic, G. Verstraete, G. Zerah, F. Jollet, M. Torrent, A. Roy, M. Mikami, Ph. Ghosez, J.-Y. Raty, D. C. Allan, Computational Material Science B., **25**, 478 (2002).

[19] P. Hohenberg, W. Kohn, Physical Review B, **136**, 864 (1964).

[20] W. Kohn, L. J. Sham, Physical Review A, **140**, 1133 (1965).
[21] C. Hartwigsen, S. Goedecker, J. Hutter, Physical Review B., **58**, 3641 (1998).
[22] D. M. Ceperley, B. J. Alder, Phys. Rev. Lett., **45**, 566 (1980).
[23] H. J. Monkhorst, J. D. Pack, Physical Review B., **13**, 5188 (1976).
[24] A. J. Smith, P. E. Meek, W. J. Liang, Journal of Physics C., **10**, 1321 (1977).

---

[*] Corresponding author: crystal_lab457@yahoo.com